A novel dry powder inhaler: Effect of device design on dispersion performance

Parthiban Selvam [a], Doug McNair [b], Randall Truman [c], Hugh D.C. Smyth [a,*]

[a] College of Pharmacy, University of Texas at Austin, Austin 78741, TX, United States
[b] Cerner Corporation Inc., KA, United States
[c] School of Engineering, University of New Mexico, NM, United States

ARTICLE INFO

ABSTRACT

The effect of device geometry and film characteristics on the performance of several passive flutter-induced dispersion DPI prototypes was investigated. Device resistance measurements indicated that the type of films, type of device geometry and specific device dimensions significantly affects the airflow resistance of the device. It was found that airflow resistance was positively correlated to the turbulence generated within the device. In addition, in vitro deposition studies indicated that the device geometry and film properties have a significant effect on aerosol dispersion performance. From these studies, selected prototypes were observed to have improved aerosolization performance without significant increases in device resistance. With further device design optimization, flutter induced dispersion DPI may be highly efficient mechanism for drug deaggregation and aerosolization.

© 2010 Published by Elsevier B.V.

1. Introduction

Dry powder inhalers (DPIs) are devices through which a dry powder formulation of an active drug is delivered for local or systemic effect via the pulmonary route. DPIs have a number of advantages over pressurized metered dose inhalers (pMDIs) and nebulizers (Islam and Gladki, 2008). Unlike pMDIs, DPIs avoid problems inherent in the use of propellant gases and the need for coordination of inhalation and actuation (Hickey et al., 1994). DPIs are also very portable, patient friendly, easy to use and do not require spacers (Geller, 2005).

An ideal DPI should be a device, which is simple to use, cost effective, convenient to carry, sufficient moisture protection, accurate and uniform dose delivery, deliver optimal drug particle size and high fine particle fraction (FPF) and low flow rate dependency (Islam and Gladki, 2008; Ashurst et al., 2000; Newman and Busse, 2002; Newman, 2004; Telko and Hickey, 2005; Clark, 1995; Donovan et al., 2009). In search of such a DPI device, many technologies and designs have been invented. For example, there are over 20 different DPI devices, single or multiple dose devices, breath activated and power driven, available in the market (Islam and Gladki, 2008). However, these devices have significant limitations such as flow rate dependency for breath-actuated devices, high complexity for power driven DPIs, insufficient drug deagglomeration and generally low respirable fraction delivery (Ganderton and Kaseem,

1992; Zeng et al., 1999; Louey and Stewart, 2002; Srichana et al., 1998; Crompton, 1991; Smith and Parry-Billings, 2003). These limitations in the marketed products have led to the development of more advanced DPIs in an attempt to overcome the aforementioned limitations. In fact, more than 25 new DPI products are being developed (Islam and Gladki, 2008). However most of these DPIs are active devices (requires built in energy sources), which are expensive, complex, face difficulties in manufacturability, and have a high number of moving parts.

Previously, we have described a DPI technology that bridges both passive and active designs using energy captured in the form of aerodynamic flutter to disperse respirable particles (Smyth and Truman, 2008). Flutter occurs when the fluid surrounding a structure feeds back dynamic energy into the structure instead of absorbing it, greatly intensifying the energy within the structure (Gallegos, 2008). Flow induced flutter has been studied intensively as a detrimental phenomena in examples such as airplane wing design and bridge construction (Njuguna, 2007; Meirovitch and Ghosh, 1987). In our previous studies, laser vibrometry was employed to assess flutter dynamics (frequency and acceleration) of aeroelastic films in a prototype inhaler (Gallegos, 2008; Smyth et al., 2008). These studies indicated that flutter frequency was independent of airflow rates, and the flutter characteristics could be 'tuned' by varying film properties such as film tension, mass, and length. It was also seen that the acceleration that was produced in the films under non-optimized flow regimes was very high – in some cases exceeding 120 g's (Smyth et al., 2008).

In this study, we have built on this previous work and investigated the effect of device geometry and film characteristics
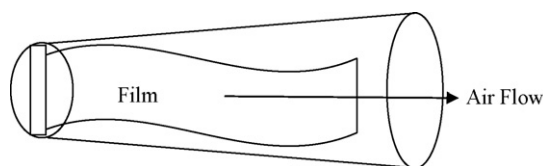
Fig. 1. Schematic view of passive flutter induced dispersion DPI.

on the performance of several passive flutter-induced dispersion DPI prototypes. In addition, we consider flutter dynamics, device airflow resistance. Our goal in these studies was to gain an understanding of how device design and inhaler resistance influenced aerosolization and dispersion performance. Our long-term hypothesis is that flutter-induced dispersion can be highly efficient for powder deaggregation and regulated to match patient, drug, and device factors (Donovan et al., 2009). The drug used in this study was ciprofloxacin. Ciprofloxacin, a member of the fluorinated quinolone family, has a wide coverage against both gram-positive and gram-negative organisms and has shown good potential as an inhaled medicine (Adi et al., 2009; Conley et al., 1997; Fitzgeorge et al., 1986). The US Food and Drug Administration (FDA) have approved orphan drug status for inhaled ciprofloxacin for pulmonary infection resulting from Pseudomonas aeruginosa infection in patients with cystic fibrosis (CF) (Waknine, 2010). Moreover, due to the extensively physicochemical characterization nature of ciprofloxacin, it could also be used as a model drug for this technology platform and will facilitate dissemination of these findings to a broader clinical development of such systems.

2. Methods

2.1. Materials

The drug ciprofloxacin was purchased from Fluka. Dow chemical company provided 4 mil Polyolefin films. CPFilms Inc. provided the transparent medical plastic film and the Polyethylene terephthalate film. An electrostatic shield film (processed polyethylene with aluminum coating) was obtained from 3M™. Methanol (99.9% assay), Glacial acetic acid (99.9% assay) and HPLC grade Acetonitrile was purchased from Fisher scientific.

2.2. Device design

Previously, a flutter-based device was employed to test drug dispersion from the coated films, wherein the flutter inducing flow was perpendicular to the axis of tension in the elastic film (Donovan et al., 2009). When the airflow is parallel to the axis of tension in a flexible film (tensioned at one end and free at the other), it still experiences flutter similar to the motion of a flag in the wind. This geometry was exploited as the drug dispersing mechanism in our prototype dry powder inhaler in these studies. An aeroelastic film coated with drug is placed in an enclosed chamber with one end tensioned, as shown in Fig. 1. The surface of the drug-coated film is parallel to the airflow, and during the inhalation process flutter is induced in the film in the direction of the airflow. Flutter dynamics in the film dislodge the drug, producing an aerosol suitable for pulmonary drug delivery.

Four different device geometries were investigated in this study. Fig. 2 illustrates the different device geometries tested. The device geometries investigated were (1) cone (inlet diameter = 0.4 cm, outer diameter = 0.6 cm, length = 3.5 cm); (2) double cone; (3) cylinder (diameter = 0.6 cm and length = 2.5 cm); (4) tapered cylinder (rectangular nozzle – 1.2 cm by 1 mm, length – 5 cm). The film dimensions used in the cone, double cone and the cylinder were
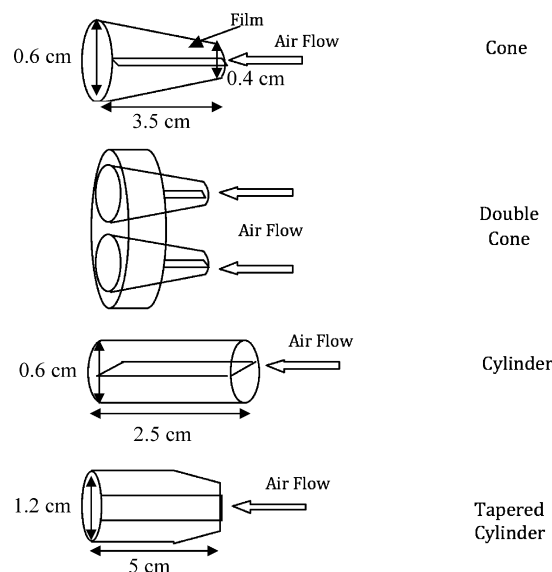

Fig. 2. Device geometries of passive flutter induced dispersion DPI prototypes.

0.3 cm in width and 2.5 cm in length. The film used in the tapered cylinder was 1.5 cm in length and 1.0 cm in width.

2.3. Drug characterization

The drug (ciprofloxacin) in the Impactor stages was washed using buffer solution (82.5:16:1.5%, v/v of methanol/Acetonitrile/glacial acetic acid) and was analyzed using a UV–vis spectrophotometer at 278 nm. Particle size analysis of micronized ciprofloxacin was performed by laser diffraction (SYMPATEC, Sympatec Gmbt, System Partikl-Technik, Germany with a He-Ne laser beam 5 mW max at 632.8 nm) using WINDOX 5.1.2 software and using scanning electron microscopy (SEM).

2.4. Flow characteristics of devices

A digital manometer recorded the pressure drop across the prototype DPI device. In this study, the flow-rate was increased from 0 to 60 lpm at 15 lpm intervals. The difference in pressure drop, determined with and without the device in place, was defined as the specific pressure drop of that device at a particular flow-rate. Each measurement was carried out in triplicate and the mean pressure drop was calculated. The mean pressure drop was plotted against the corresponding flow rate and the slope of the fitted line is reported as the device resistance (Srichana et al., 1998).

2.5. Aerosol characterization

The in vitro drug dispersion performance of the device was investigated using a Next Generation Impactor (NGI) at a flow rate of 60 L min⁻¹. The following parameters were determined from the NGI dispersion data: (1) Fine Particle Fraction (FPF) – the percentage of drug deposition from stages 3 to 8 with respect to total emitted dose (throat to stage 8); (2) Fine Particle Dose (FPD) – the amount of drug deposited in stage 3 to stage 8; (3) respirable fraction (RF) – the percentage of drug deposition from stages 3 to 8 with respect to total dose; (4) emitted dose (ED) – the amount of dose delivered by the DPI.

Table 1
Device airflow resistance as a function of the prototype DPI geometries using polyolefin films.

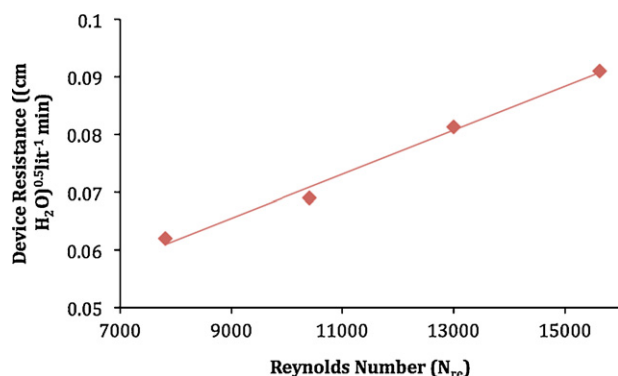| Device	Device resistance ((cm of H_2O)$^{0.5}$ L^{-1} min)	RF (%)
Double cone	0.095	26.4 ± 1.4
Cylinder	0.102	31.1 ± 2.2
Tapered cylinder	0.126	41.3 ± 2.1
Cone	0.169	46.0 ± 3.5

Fig. 3. Device airflow resistance (without film) as a function of the Reynolds number of airflow.

Table 2a
Device airflow resistance for the prototype geometries with and without polyolefin films.

Device	Device resistance ((cm of H_2O)$^{0.5}$ L^{-1} min)	
	Without film	With film
Double cone	0.062	0.095
Cylinder	0.069	0.102
Tapered cylinder	0.081	0.126
Cone	0.091	0.169

3. Results

3.1. Device resistance measurements

Device airflow resistance measurements are important for device design and comparing performance between different devices. Here we assessed device resistance as a function of device design and the type of film loaded into the device.

3.1.1. Effect of device geometry

Table 1 shows airflow resistance values for the different device geometries tested in these studies. These resistance values span a typical spectrum observed in currently marketed devices. In Fig. 3 we have calculated the Reynolds number for each device and correlated it with device resistance. As expected, by manipulating the device geometry increases in the airflow resistance of the device led to increases in the turbulence (Reynolds number). In Table 2,

Table 2b
Device airflow resistance as a function of the films in cone geometry.

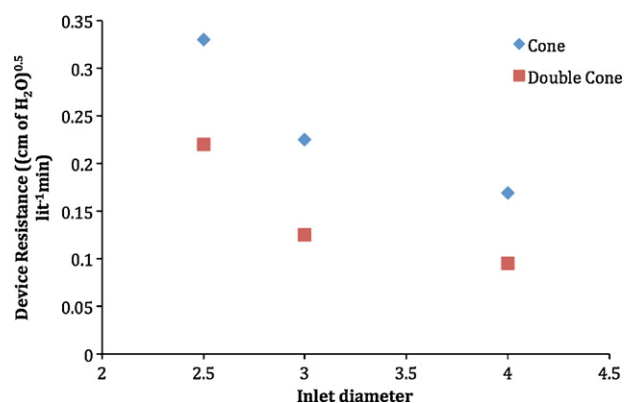|	Description	Film Thickness (μm)	Device resistance ((cm of H_2O)$^{0.5}$ L^{-1} min)
Film 1	Polyolefin medical film	85 ± 4	0.169
Film 2	Transparent window film	98 ± 3	0.181
Film 3	PET film	109 ± 2	0.204
Film 4	Metalized polyethylene	120 ± 5	0.224

Fig. 4. Device airflow resistance as a function of the device dimensions of the cone and double cone prototype DPI geometries using polyolefin films.

the device airflow resistance is correlated to the aerosol dispersion performance of the device geometry (with film). The film used in this study is a polyolefin film and *in vitro* dispersion study was performed at 60 lpm. The double cone which has the least resistance of 0.095 (cm of H_2O)$^{0.5}$ L^{-1} min also had the lowest device performance as measured by respirable fraction (RF = 26.4 ± 1.4%). The cone geometry prototype had the highest device resistance of 0.169 (cm of H_2O)$^{0.5}$ L^{-1} min and produced the highest dispersion performance with a RF of 46.0 ± 3.5%. In these prototypes, increasing the device resistance by manipulating the device geometry increased the device dispersion performance.

3.1.2. Effect of films

To study the effect of films on device resistance, resistance measurements were performed using the cone-geometry prototype DPI device across several different film types (Table 2b). As expected, Table 2a shows that the device airflow resistance increased in the presence of the polyolefin film for all the geometries. There was also significant impact of the film type on airflow resistance. For the cone geometry prototype device, as the film thickness increases the resistance also increases. The polyolefin film having a thickness of 85 μm provided the least resistance of 0.169 (cm of H_2O)$^{0.5}$L^{-1} min, while the metalized polyethylene film (120 μm) produced a device resistance of 0.224 (cm of H_2O)$^{0.5}$ L^{-1} min.

3.1.3. Effect of device dimensions

Fig. 4 represents the device resistance as a function of the inlet diameter of the cone and double cone geometry. The measurements were performed using polyolefin films inserted in the device and the angle of opening of the device geometries was kept constant. Increasing the inlet diameter from 0.25 to 0.4 cm, the device resistance is decreased for both the geometries. The device resistance is lower for the double cone geometry than the single cone geometry for corresponding inlet diameters.

3.2. Aerosolization performance

Performance of dry powder inhalers was assessed using standard pharmacopeial methods. We assessed the overall efficiency of dispersion (RF), the efficiency of detachment of the drug from the films (percentage emitted, ED), the efficiency of the deaggregation of the detached drug (Fine particle fraction, FPF), and also normalized this efficiency for surface area of film used (FPD/cm^2). These performance measures were assessed across a range of device geometries (as described above) and as a function of several film properties.

Table 3
Aerosol properties of various prototype DPI geometries determined using NGI.

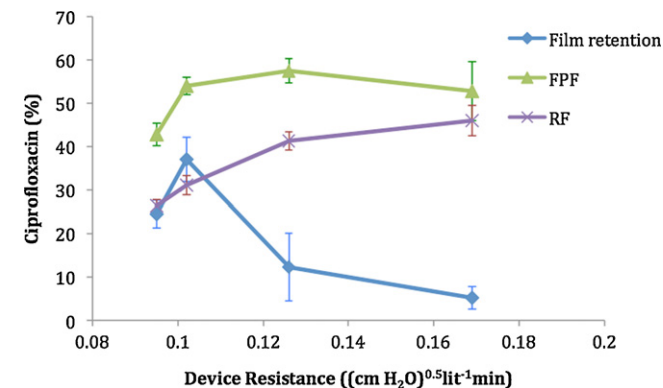| Geometry	FPF (%)	RF (%)	ED (%)	FPD/area (μg cm^{-2})
Cone	52.8 ± 6.8	46.0 ± 3.5	87.6 ± 5.2	66.8 ± 16.7
Double cone	42.8 ± 2.6	26.4 ± 1.4	61.7 ± 3.2	33.5 ± 3.4
Cylinder	54.0 ± 2.0	31.1 ± 2.2	57.6 ± 2.4	45.6 ± 11.1
Tapered cylinder	57.5 ± 2.8	41.3 ± 2.1	71.9 ± 1.9	88.3 ± 5.6

Fig. 5. Effect of prototype device geometry – aerosol dispersion profile determined by NGI using polyolefin films ($n = 3$).

3.2.1. Effect of device geometry

Based on observations from the device resistance studies above, the film used in the remainder of the studies was the polyolefin film. As seen in Table 3, the aerosol performance was significantly influenced by the device geometry. The percentage emitted (ED) is statistically similar at lower resistances (double cone and cylinder device geometry) and increases with increasing resistance. The ED for cone geometry having the highest resistance of 0.169 (cm of H$_2$O)$^{0.5}$ L^{-1} min) was 87.6%. From Fig. 5, it was clear that the film retention was highest for the cylinder geometry at 37%. In general film retention of the drug particles decreased with increasing airflow device resistances. Fine particle fraction (FPF) and respirable fraction (RF) increases initially with increasing airflow device resistance and then reaches a plateau at around 0.11 (cm of H$_2$O)$^{0.5}$ L^{-1} min. The cylinder geometry had the highest FPF of 57.5% while the cone geometry has the highest RF of 46%. The double cone geometry has the lowest RF and FPF of 26.4% and 42.8%, respectively.

3.2.2. Effect of film dimensions

Based on the effects of the device geometry on resistance and performance obtained from the studies already described, the tapered cylinder device was chosen for the next experiments that aimed to determine the effects of the film dimensions on DPI performance.

(a) Effect of length: The polyolefin film used in this study had film lengths of 3 and 1.5 cm, and film width of 1.5 cm. As indicated from Table 4 and Fig. 6, aerosol dispersion efficiencies from the 1.5 cm film was significantly greater than its 3 cm counterpart. A higher RF of 41.29 ± 2.06% was achieved with the shorter film length compared to 27.3 ± 2.5% for 3 cm film. The film retention and throat deposition was higher for the longer film (3 cm), but, as the film contained more drug, this longer film had a higher FPD

Table 4
Aerosol properties of tapered cylinder geometry of varying film lengths using NGI.

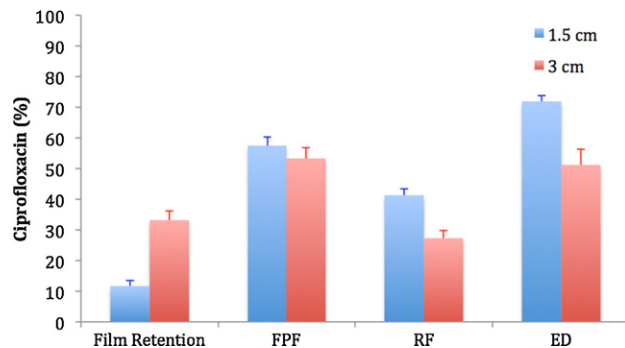| Film length	FPF (%)	RF (%)	ED (%)	FPD (μg)
1.5 cm	57.5 ± 2.8	41.3 ± 2.1	71.9 ± 1.9	198.8 ± 12.5
3 cm	53.3 ± 3.5	27.3 ± 2.5	51.2 ± 5.1	289.7 ± 17.3

Fig. 6. Effect of film length – aerosol dispersion profile determined by NGI using polyolefin films ($n = 3$).

Table 5
Aerosol properties of tapered cylinder geometry of varying film lengths using NGI.

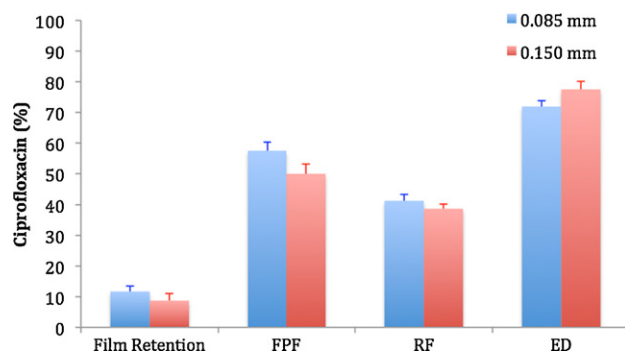| Film thickness	FPF (%)	RF (%)	ED (%)	Film retention (%)
0.085 mm	57.5 ± 2.8	41.3 ± 2.1	71.9 ± 1.9	11.7 ± 1.8
0.150 mm	50.0 ± 3.2	38.7 ± 1.5	77.5 ± 2.6	8.74 ± 2.3

Fig. 7. Effect of film thickness – aerosol dispersion profile determined by NGI using polyolefin films ($n = 3$).

of 289.73 ± 17.27 μg compared to 198.8 ± 12.5 of the shorter film (1.5 cm) (Table 5).

(b) Effect of film thickness: Two thicknesses of the polyolefin films were studied: 0.15 and 0.085 mm. As above, the prototype design used in this study was the tapered cylinder geometry. As the thickness of the film was increased, the aerosol dispersion performance of the device was not significantly different. However as the thickness of the film was increased, the resistances of the devices significantly increased from 0.126 to 0.240. Even though film retention is higher for the 0.085 mm film compared to 0.15 mm film, the FPF is higher for 0.085 mm film (57.5 ± 2.8%) compared to 0.15 mm film (50.0 ± 3.2%) (Fig. 7).

4. Discussion

4.1. Device resistance measurements

The airflow resistance of the device is an important parameter to consider when designing a novel device. It should not be insuffi-

cient to capture the energy of inhalation or sufficiently elevated to prevent those with poor lung function from using the device.

4.1.1. Effect of films

In this study, it could be seen that the type of films affects the device resistance. This is due to the intrinsic physical properties of the film (Moretti, 2003) and the thickness (mass ratio) of the films (Connell and Yue, 2007). The polyolefin film, which resulted in the least device resistance, was selected as the lead candidate of the films studied here. The increase in the device airflow resistance in the presence of film is due to the resistance to the airflow offered by the film in the form of flutter. We postulate that the presence of these fluttering films would further increase the turbulence (higher Reynolds number) and may help to deaggregate the aerosolized drug. Moreover, the turbulence generated at 60 lpm ($7800 < N_{re} < 15,600$) using these flutter induced dispersion DPI geometries is higher than the commercially available in the market. For example, at the narrowest exit point of the Spinhaler, the N_{re} is approximately 13,000 at 120 lpm and 3250 at 30 lpm (French et al., 1996).

4.1.2. Effect of geometry

The geometry of the device significantly affects the device resistance and the aerosol dispersion performance. Higher resistance devices generally produce higher turbulence (Srichana et al., 1998), and it may be expected, in our case, to increase the flutter intensity and lead to a higher RF. The FPF of a high resistance devices available in the market such as Inhalator (0.180 (cm of $H_2O)^{0.5} L^{-1}$ min) is around 25% at 60 lpm. In comparison, the highest resistance device geometry studied here, i.e. the cone geometry, had a FPF of around 50% and, due to differences in flutter performance, a lower resistance device (tapered cylinder) had an even higher FPF (57.5%). Similarly, the FPF of a low resistance device available in the market such as Rotahaler (0.04 (cm of $H_2O)^{0.5} L^{-1}$ min) is around 15–20% (Srichana et al., 1998). This FPF was lower than the lowest resistance device geometry studied here, i.e. the double cone geometry that had a FPF of around 40%.

4.1.3. Effect of device dimensions

The dimensions (especially the internal diameter) of the cone geometry and the double cone geometry significantly affect the device resistance. This may be due to increased turbulence that would be associated with the decrease in internal diameter of the device. As described above, increases in turbulence may affect flutter dynamics (onset and intensity), hence, will affect drug dispersion performance. However the nature of flutter dynamics and its relationship with the device geometry and dimensions are yet to be fully understood in our case and even in well developed areas of flutter research due to the complexity of the interactions between the air flow and the dynamic structure undergoing flutter (Meirovitch and Ghosh, 1987; Njuguna, 2007).

4.2. Aerosolization performance

4.2.1. Effect of device geometry

Device geometries such as cylinder and double cone, having low resistances, give rise to high drug retention on the film during cascade impaction studies. On the other hand, high-emitted dose percentages are found in both the cone and tapered geometries, where the device resistance is greater and the device geometries are in closer distance to the drug loaded film. This would indicate for these conditions, flow velocities and turbulence are important for inducing detachment.

In contrast to detachment, deaggregation appears to be less dependent on the device resistance. The FPF and RF values remain relatively constant after a device airflow resistance of 0.11 (cm of $H_2O)^{0.5} L^{-1}$ min) is obtained across the different device designs. Even though the aerosol performance (RF) is enhanced in both of the higher resistance designs, the cone geometry exhibited the highest throat deposition. This suggests that the tapered cylinder design was the best candidate among the different geometries studied. The tapered cylinder geometry, which has a comparable device resistance to the turbuhaler, has a better device performance (Thorsson et al., 1994; Crompton, 1991; Ball et al., 2002). This indicates that the passive flutter induced dispersion DPI device is a significantly better product compared to the commercially available DPI products. In on going studies, we are performing controlled studies using a statistical design of experiment that focuses on the tapered cylinder design.

4.2.2. Effect of film dimensions

The film properties also affect the aerosol performance of the device. Shorter film tends to reduce film retention and increase dispersion at the expense of FPD. The FPD dose is higher in the longer film. The FPF and RF is lower for the 0.15 mm thick film, suggesting that the film is more rigid at higher thicknesses, resulting in lower magnitude flutter forces at a constant flow rate. The FPD delivered using this device is greater than the commercially available DPI products (Bisgaard et al., 1998).

5. Conclusions

The effect of device geometry and film characteristics on the device airflow resistance and aerosolization performance of the passive flutter induced dispersion DPI prototypes was studied. Device resistance measurements indicate that the type of films, type of device geometry and specific device dimensions significantly affects the airflow resistance of the device. In addition, aerosol dispersion performance studies indicated that the device geometry and film properties significantly affect the aerosol performance of the device. These studies indicate that with further device design optimization, flutter induced dispersion DPI may be highly efficient mechanism for drug deaggregation and aerosolization.

References

Adi, H., et al., 2009. Controlled release antibiotics for dry powder lung delivery. Drug Dev. Ind. Pharm. 36, 119–126.

Ashurst, I., et al., 2000. Latest advances in the development of dry powder inhalers. Pharm. Sci. Technol. Today 3, 246–256.

Ball, D.J., et al., 2002. Deposition and pharmacokinetics of budesonide from the Miat Monodose inhaler, a simple dry powder device. Int. J. Pharm. 245, 123–132.

Bisgaard, H., et al., 1998. Fine particle mass from the Diskus inhaler and Turbuhaler inhaler in children with asthma. Eur. Respir. J.: Official J. Eur. Soc. Clin. Respir. Physiol. 11, 1111–1115.

Clark, A.R., 1995. Medical aerosol inhalers: past, present, and future. Aerosol Sci. Technol. 22, 374–391.

Conley, J., et al., 1997. Aerosol delivery of liposome-encapsulated ciprofloxacin: aerosol characterization and efficacy against Francisella tularensis infection in mice. Antimicrob. Agents Chemother. 41, 1288–1292.

Connell, B.S.H., Yue, D.K.P., 2007. Flapping dynamics of a flag in a uniform stream. J. Fluid Mech. 581, 33–67.

Crompton, G.K., 1991. Dry powder inhalers: advantages and limitations. J. Aerosol Med.: Official J. Int. Soc. Aerosol Med. 4, 151–156.

Donovan, M., et al., 2009. Tunable dry powder inhalers: future or folly? Respir. Drug Deliv. 1, 189–200.

Fitzgeorge, R.B., et al., 1986. Treatment of experimental legionnaires-disease by aerosol administration of rifampicin, ciprofloxacin, and erythromycin. Lancet 1, 502–503.

French, D.L., Edwards, D.A., Niven, R.W., 1996. The influence of formulation on emission, deaggregation and deposition of dry powders for inhalation. J. Aerosol Sci. 27, 769–783.

Gallegos, M., 2008. Flow Induced Flutter of Thin Elastic Films. University of New Mexico, M.S. Albuquerque, NM.

Ganderton, D.J., Kaseem, N.M., 1992. Dry powder inhaler. In: Advances in Pharmaceutical Sciences. Academic Press, London, pp. 165–191.

Geller, D.E., 2005. Comparing clinical features of the nebulizer, metered-dose inhaler, and dry powder inhaler. Respir. Care 50, 1313–1321, discussion 1321–1322.

Hickey, A.J., et al., 1994. Factors influencing the dispersion of dry powders as aerosols. Pharm. Technol. 8, 58–82.

Islam, N., Gladki, E., 2008. Dry powder inhalers (DPIs) – a review of device reliability and innovation. Int. J. Pharm. 360, 1–11.

Louey, M.D., Stewart, P.J., 2002. Particle interactions involved in aerosol dispersion of ternary interactive mixtures. Pharm. Res. 19, 1524–1531.

Meirovitch, L., Ghosh, D., 1987. Control of flutter in bridges. J. Eng. Mech. 113, 720–736.

Moretti, P.M., 2003. Tension in fluttering flags. In Tenth International Congress on Sound and Vibration. Stockholm, Sweden.

Newman, S.P., Busse, W.W., 2002. Evolution of dry powder inhaler design, formulation, and performance. Respir. Med. 96, 293–304.

Newman, S.P., 2004. Dry powder inhalers for optimal drug delivery. Expert Opin. Biol. Ther. 4, 23–33.

Njuguna, J., 2007. Flutter prediction, suppression and control in aircraft composite wings as a design prerequisite: a survey. Struct. Control Health Monit. 14, 715–758.

Smith, I.J., Parry-Billings, M., 2003. The inhalers of the future? A review of dry powder devices on the market today. Pulm. Pharm. Ther. 16, 79–95.

Smyth, H.D.C., Gallegos, M., Truman, R.C., 2008. A novel mechanism of dry powder inhaler dispersion: optimizing flow induced flutter. Respir. Drug Deliv. 3, 877–880.

Smyth, H.D.C., Truman, R.C., 2008. Dry powder Inhaler with Aeroelastic dispersion mechanism, EP20070752039.

Srichana, T., Martin, G.P., Marriott, C., 1998. Dry powder inhalers: the influence of device resistance and powder formulation on drug and lactose deposition in vitro. Eur. J. Pharm. Sci. 7, 73–80.

Telko, M.J., Hickey, A.J., 2005. Dry powder inhaler formulation. Respir. Care 50, 1209–1227.

Thorsson, L., Edsbacker, S., Conradson, T., 1994. Lung deposition of budesonide from Turbuhaler is twice that from a pressurized metered-dose inhaler P-MDI. Eur. Respir. J. 7, 1839–1844.

Waknine, Y., 2010. FDA Approves Orphan Drug Status for Inhaled Ciprofloxacin for Cystic Fibrosis. Medscape Today.

Zeng, X.M., et al., 1999. Effects of particle size and adding sequence of fine lactose on the deposition of salbutamol sulphate from a dry powder formulation. Int. J. Pharm. 182, 133–144.